Regulation of Terminal Schwann Cell Number at the Adult Neuromuscular Junction

Jane L. Lubischer and David M. Bebinger

Section of Neurobiology, School of Biological Sciences, Institute for Neuroscience and Institute for Cellular and Molecular Biology, University of Texas, Austin, Texas 78712

Terminal Schwann cells (TSCs), neuroglia that cover motoneuron terminals, play a role in regulating the structure and function of the neuromuscular junction. In rats, the number of TSCs at each junction increases rapidly in early postnatal life and more slowly in young adults. It is possible that TSC number increases to match increasing endplate area. Alternatively, the increase in TSC number may reflect a developmental process independent of endplate size or terminal function. To experimentally test the relationship between endplate size and TSC number, we manipulated endplate area in an androgen-sensitive muscle of the rat, the levator ani (LA), by castration and by androgen replacement. We found that TSC number not only increased as endplates enlarged but also decreased when endplates shrank. Ninety days after castration, TSC number decreased by ∼20% (one cell per junction) as endplate size decreased by 30%. These effects were reversed by testosterone. Testosterone levels did not affect TSC number in the extensor digitorum longus (EDL) muscle, where endplate area was unaffected by castration or testosterone treatment. TSC number was, however, significantly correlated with endplate area in both LA and EDL muscles. Furthermore, the relationship between endplate size and TSC number, as defined by the slope of the regression line, was the same in LA and EDL muscles, indicating that this relationship is not a unique feature of the LA muscle. These data suggest that TSC number is a dynamic property of the neuromuscular synapse that is actively regulated throughout life.

Key words: NMJ; SNB; motoneuron; steroid hormone; synaptic plasticity; perisynaptic Schwann cells

Neuroglial cells are now known to play an active role in the development and function of neurons in both the central and peripheral nervous systems. In the CNS, glial cells influence synaptogenesis, maintain a close physical association with synapses, respond to neurotransmitters, release glutamate and ATP, and modify synaptic transmission (Pfrieger and Barres, 1996; Araque et al., 1999). At the neuromuscular junction (NMJ), nonmyelinating terminal Schwann cells (TSCs) cover all nerve terminal branches. These cells not only play an important role in synaptic stability and nerve growth (Ko and Chen, 1996; Son et al., 1996; Trachtenberg and Thompson, 1997; Lubischer and Thompson, 1999) but also respond to neurotransmitters (Jahromi et al., 1992; Reist and Smith, 1992) and modulate synaptic transmission (Robitaille, 1998).

During early postnatal development, the number of TSCs per NMJ increases dramatically (Love and Thompson, 1998). If these cells are important to the normal functioning of this synapse, one might expect to see a regulation of the number of TSCs in response to changes of the NMJ during adult life. To address the question of whether TSC number is regulated in adult animals, we took advantage of a highly steroid-sensitive neuromuscular system

to manipulate terminal size by altering testosterone levels. The levator ani (LA) and bulbocavernosus (BC) muscles respond to experimental or seasonal changes in circulating testosterone levels with dramatic changes in muscle fiber size (Forger and Breedlove, 1987; Bleisch and Harrelson, 1989). Other muscles, such as the extensor digitorum longus (EDL), express lower levels of androgen receptors (Rance and Max, 1984) and are much less responsive to testosterone (Wainman and Shipounoff, 1941). After castration of adult rats or mice, LA and BC muscle fibers atrophy, and there is a corresponding decrease in the size of NMJs, both presynaptically and postsynaptically (Bleisch and Harrelson, 1989; Balice-Gordon et al., 1990). Treating castrates with testosterone reverses these changes. We now present evidence that the number of TSCs present at NMJs in LA muscles changes in coordination with terminal size after castration and after testosterone replacement therapy.

Parts of this paper have been published previously in abstract form (Bebinger et al., 1998).

This article is published in *The Journal of Neuroscience*, Rapid Communications Section, which publishes brief, peer-reviewed papers online, not in print. Rapid Communications are posted online approximately one month earlier than they would appear if printed. They are listed in the Table of Contents of the next open issue of JNeurosci. Cite this article as: JNeurosci, 1999, 19:RC46 (1–5). The publication date is the date of posting online at www.jneurosci.org.

http://www.jneurosci.org/cgi/content/full/3776

Table 1. Testosterone regulates LA muscle weight and fiber cross-sectional area (mean ± SEM)

	Muscle weight (mg)	Fiber CSA (μm^2)
Normal ($t = 0$)	228 ± 17.6 ($n = 3$)	2298 ± 151.3 ($n = 4$)
Sham ($t = 90$ d)	207 ± 12.5 (6)	2376 ± 161.2 (6)
Castrate ($t = 90$ d)	101 ± 10.3* (6)	1054 ± 125.1* (6)
Sham + blank ($t = 180$ d)	227 ± 10.2 (6)	2476 ± 141.0 (6)
Castrate + blank ($t = 180$ d)	92 ± 4.7* (6)	757 ± 57.2* (6)
Castrate + testosterone ($t = 180$ d)	279 ± 12.4** (6)	3212 ± 179.1** (6)

Measurements were made in normal animals ($t = 0$), in animals castrated (Castrate) or sham-castrated (Sham) for 90 d ($t = 90$ d), and in animals castrated or sham-castrated for 90 d and then given testosterone or blank implants for another 90 d ($t = 180$ d). Sample sizes are in parentheses. Fiber cross-sectional areas (CSA) are based on 50 fibers per muscle.

*Significantly smaller than groups with testosterone present; $p < 0.0001$.

**Significantly larger than all other groups; $p < 0.01$.

MATERIALS AND METHODS

Adult male Wistar rats purchased from Harlan Sprague Dawley (Indianapolis, IN) were housed in the Animal Resources Center at the University of Texas at Austin. Surgical procedures were performed on animals anesthetized with ether. Measurements were made at three time points: $t = 0$, 90, or 180 d. At $t = 0$ d, animals weighing at least 390 gm were killed by overdose for baseline measurements ($n = 4$), castrated, or sham-castrated. Ninety days later ($t = 90$ d), animals were killed ($n = 6$) or given implants; castrated animals were given either testosterone-filled or blank implants, and shams were given blank implants ($n = 6$ per group). Implants were replaced after 45 d, and animals were killed after another 45 d, for a total of 90 d of hormone treatment ($t = 180$ d). Testosterone implants (effective release length, 60 mm) were made by packing testosterone (4-androsten-17β-ol-3-one; T-1500, Sigma, St. Louis, MO) into silicone tubing (1.59 mm inner diameter and 3.2 mm outer diameter; Konigsberg Instruments, Pasadena, CA), plugging the ends with wooden dowels, and sealing with SILASTIC adhesive (Dow Corning, Midland, MI). After soaking in 0.01 M phosphate buffer overnight, implants showing signs of leakage were discarded. Implants made in this way result in plasma levels of testosterone that approximate those found in normal adult male rats (Smith et al., 1978). Blank implants were made in the same way but left empty.

LA and EDL muscles were dissected into oxygenated Ringer's solution, blotted dry, and weighed. Right and left LA muscles were separated by cutting along the midline raphe where they are attached. One LA and EDL muscle from each animal were frozen in isopentane cooled to between −80 and −90°C with liquid nitrogen and cryostat-sectioned at −20°C at the level of the endplate band [verified by α-bungarotoxin labeling of acetylcholine receptors (AChRs)]. Sections 10 μm thick were stained with 1% methylene blue (12 min), rinsed in PBS (two times for 3 min each), and coverslipped under Gel/Mount (Biomeda, Foster City, CA). Muscle fiber cross-sectional area was measured on photographs taken using a 63×, 1.32 numerical aperture objective, an integrated, cooled CCD camera (Zeiss, Thornwood, NY), and NIH Image software. Ten fibers were sampled from each of five regions of the cross section, for a total of 50 fibers per muscle.

The contralateral LA and EDL muscles were processed for immunohistochemical labeling of NMJs (Lubischer and Thompson, 1999). Briefly, muscles were fixed in 4% paraformaldehyde, permeabilized in absolute MeOH cooled to −20°C, and labeled with the following antibodies: a rabbit polyclonal to S100 to visualize Schwann cells (1:400; Z0311, Dako, Glostrup, Denmark), a mouse monoclonal to neurofilament (2H3) to visualize axons (1:200; Developmental Studies Hybridoma Bank, University of Iowa, Iowa City, IA), a mouse monoclonal to the synaptic vesicle protein SV2 to visualize nerve terminals (1:500; Developmental Studies Hybridoma Bank), fluorescein isothiocyanate-conjugated goat anti-rabbit (1:400; 55659, Cappel, West Chester, PA), and Cy5-conjugated sheep anti-mouse (1:100; Jackson ImmunoResearch, West Grove, PA). AChRs were visualized using tetramethylrhodamine isothiocyanate-conjugated α-bungarotoxin. Cell nuclei were labeled using 4,6-diamidino-2-phenylindole (DAPI; 0.1 μg/ml for 8 min). At least 40 junctions were sampled per LA (mean, 46), and 30 per EDL (mean, 39). For each junction, TSCs were counted, and AChR plaques were photographed. Endplate area was determined using NIH Image software to invert the digital image, convert it to binary, and adjust the threshold to give a binary image that matched the original; the software

Table 2. Testosterone does not regulate EDL muscle weight or fiber cross-sectional area (mean ± SEM)

	Muscle weight (mg)	Fiber CSA (μm^2)
Sham ($t = 90$ d)	252 ± 6.9	3094 ± 78.4
Castrate ($t = 90$ d)	263 ± 8.8	3220 ± 179.4
Sham + blank ($t = 180$ d)	320 ± 12.7*	3407 ± 126.6
Castrate + blank ($t = 180$ d)	279 ± 12.7	3461 ± 182.5
Castrate + testosterone ($t = 180$ d)	288 ± 9.0**	3325 ± 167.7

Measurements were made in animals ($n = 6$ per group) that were castrated (Castrate) or sham-castrated (Sham) for 90 d ($t = 90$ d) and in animals that had been castrated or sham-castrated for 90 d and then given testosterone or blank implants for another 90 d ($t = 180$ d). Fiber cross-sectional areas (CSA) are based on 50 fibers per muscle. Fiber CSA did not differ among groups. Muscle weight varied but was not related to testosterone levels. There were no differences among groups when muscle weight was considered relative to body weight (data not shown).

*Significantly larger than all other groups; $p < 0.05$.

**Significantly larger than Sham; $p < 0.05$.

then computed the number of black pixels and converted this to an area based on calibration with a stage micrometer. Measures of endplate area accurately reflect terminal size because of the precise apposition of presynaptic and postsynaptic elements (Rich and Lichtman, 1989; Balice-Gordon et al., 1990).

Statistical analyses, run separately for LA and EDL muscles, were performed using StatView (SAS Institute, Cary, NC) as one-way ANOVAs, with hormonal condition as the between-group factor. Significant effects were followed by hypothesis-driven *post hoc* comparisons using Fisher's protected least significant difference. Analyses of correlations used the Pearson product–moment correlation coefficient. Data are presented as mean ± SEM.

RESULTS

To test the effects of castration, we made measurements in normal adult males ($t = 0$ d) and in males 90 d after they had been castrated or sham-castrated ($t = 90$ d). To determine whether the effects of castration could be reversed by testosterone, we implanted animals 90 d after castration with testosterone-filled or blank implants and made measurements after a further 90 d ($t = 180$ d). As previously reported (Bleisch and Harrelson, 1989), LA muscle weight and fiber cross-sectional area were extremely sensitive to testosterone levels (Table 1). Both decreased by >50% 90 d after castration and returned to or exceeded normal levels after a further 90 d of replacement testosterone treatment. There were no such testosterone-dependent changes in EDL muscle weight or fiber cross-sectional area (Table 2). One group of gonadally intact animals had larger EDLs than the other groups, but this was related to body weight and not to testosterone levels.
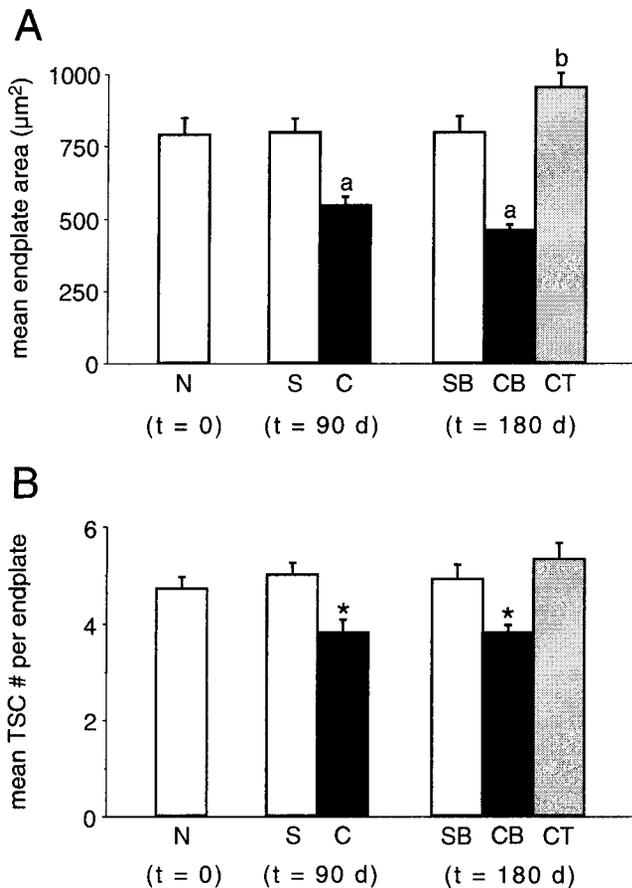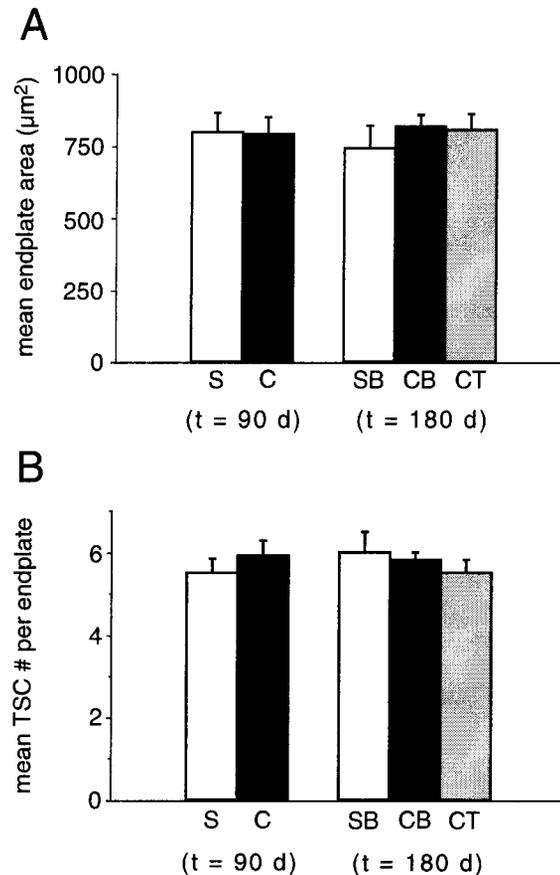
Figure 1. Testosterone regulates endplate area and TSC number in LA muscles. Mean endplate area (*A*) and TSC number (*B*) are given for normal rats (*N*) at the beginning of the experiment (*t* = 0), in rats at *t* = 90 d that were castrated (*C*) or sham-castrated (*S*) at *t* = 0, in rats at *t* = 180 d that were castrated (*CB*) or sham-castrated (*SB*) at *t* = 0 and given blank implants between *t* = 90 and 180 d, or in rats that were castrated at *t* = 0 and given testosterone implants between t = 90 and 180 d (*CT*). *Bars* are shaded to indicate equivalent hormonal conditions: *white* for gonadally intact animals with normal testosterone levels, *black* for castrates given no testosterone treatment, and *gray* for animals castrated and then given replacement testosterone therapy. *A,* Both castrate groups (*black*) had smaller endplates than normals or shams (*white*). After testosterone treatment (*gray*), endplate area was larger than normal. [a]Significantly different from normals and shams (*p* < 0.001); [b]significantly different from all other groups (*p* < 0.02). *B,* TSC number was lower in castrates (*) than in normals (*p* < 0.05), sham castrates (*p* < 0.01), or castrates treated with testosterone (*p* < 0.001). At least 40 junctions were sampled from each muscle in four normal animals and in six animals in all other groups.

After correcting for body weight, there were no differences among groups for EDL weight and no change in the effects of castration and testosterone on LA weight.

Testosterone regulates junction size and TSC number in LA muscles

As expected (Bleisch and Harrelson, 1989; Balice-Gordon et al., 1990), reduction of LA fiber size by castration caused a decrease in endplate area (Fig. 1*A*). Mean LA endplate area was 70% of normal 90 d after castration. Like LA muscle weight and fiber cross-sectional area, endplate area increased to slightly greater than normal after 90 d of testosterone replacement therapy. There were no such changes in the size of EDL endplates (Fig. 2*A*).

Figure 2. Testosterone does not regulate endplate area or TSC number in EDL muscles. Mean endplate area (*A*) and TSC number (*B*) are given for rats castrated (*C*) or sham-castrated (*S*) for 90 d, castrated for 90 d and then given blank implants for 90 d (*CB*), sham-castrated for 90 d and then given blank implants for 90 d (*SB*), or castrated for 90 d and then given testosterone implants for 90 d (*CT*). *Bars* are shaded as in Figure 1 to indicate equivalent hormonal conditions. At least 30 junctions were sampled from each muscle in five animals per group at *t* = 90 d and six animals per group at *t* = 180 d.

As fiber size and endplate area changed in LA muscles, TSC number also changed (Figs. 1*B*, 3). TSCs were identified as cells over the terminal that were S100-positive (Fig. 3*B,E*) and contained a DAPI-labeled nucleus (Fig. 3*C,F*). After castration, mean TSC number at LA endplates decreased by approximately one cell (a 20% decrease). After 90 d of testosterone treatment, mean TSC number returned to slightly above normal, although not enough to become significantly different from gonadally intact controls. That testosterone treatment resulted in a significant rebound in endplate size without a significant increase in TSC number over normal probably reflects the fact that endplate area can vary continuously, whereas TSC number is a discrete variable. There were no changes in TSC number in EDL muscles under the different hormonal conditions (Fig. 2*B*), and we did not see any obvious effects of testosterone levels on TSC morphology in either muscle.

TSC number correlates with junction size in both the LA and the EDL

Mean TSC number was correlated with mean endplate area in both LA (r^2 = 0.665; *p* < 0.0001) and EDL (r^2 = 0.375; *p* < 0.001) muscles (Fig. 4). The relationship between endplate area and TSC number, as defined by the slope of the regression line,

Figure 3. NMJs in LA muscles from animals lacking testosterone were smaller and had fewer TSCs than those from normal animals or castrates given testosterone replacement therapy. Junctions were triple-labeled to visualize AChRs (*A, D*), Schwann cells (*B, E*), and cell nuclei (*C, F*). *A–C,* Fluorescence photomicrographs of an NMJ from an animal sham-castrated 180 d earlier. This junction had an endplate area of 812 μm^2 and six TSCs (*B, C, arrows*). *D–F,* Fluorescence photomicrographs of an NMJ from an animal castrated 180 d earlier.

This junction had an endplate area of 657 μm^2 and four TSCs (*E, F, arrows*). Photos were chosen to illustrate TSC number; there was no difference between groups in apparent AChR labeling intensity. Scale bar, 10 μm.
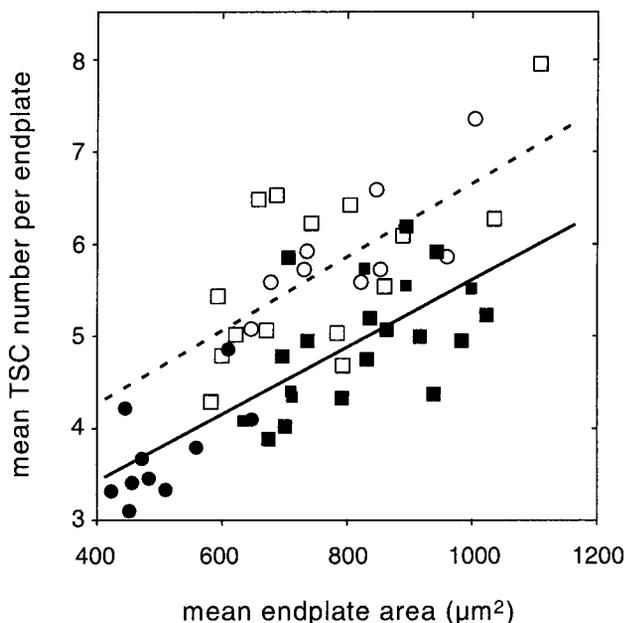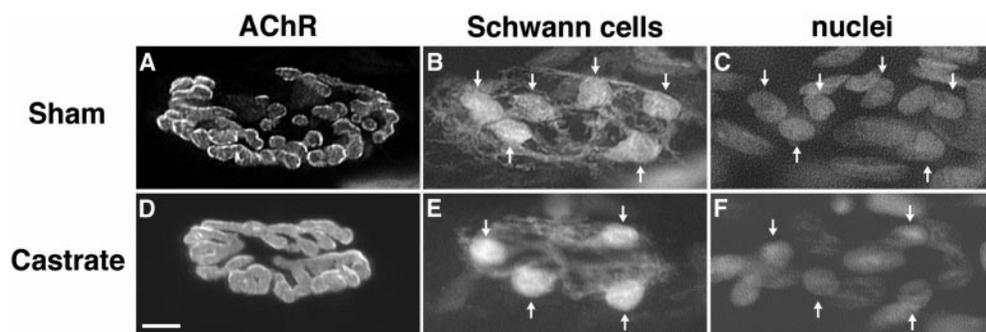
Figure 4. TSC number is correlated with endplate size in both LA ($r^2 = 0.665$; $p < 0.0001$) and EDL ($r^2 = 0.375$; $p < 0.001$) muscles. Mean TSC number per endplate is plotted against mean endplate area for each animal. *Solid symbols* represent LA muscles, and *open symbols* represent EDL muscles. *Squares* indicate animals with testosterone present, either endogenous (shams) or exogenous (those given implants). *Circles* indicate animals that had been castrated for 90 or 180 d without testosterone treatment. The *upper, dotted line* is the regression line for EDL muscles, and the *lower, solid line* is the regression line for LA muscles. The two lines have the same slope.

was the same for both muscles, although junctions in EDL muscles had, on average, approximately one more TSC than did junctions in LA muscles. In both muscles, there was an increase of approximately one TSC for every increase of 250 μm^2 in endplate area. When the correlation between endplate area and TSC number was tested within each animal, 29 of 30 LA muscles exhibited a significant correlation ($p < 0.01$). Regression lines were fit to these data, and their slopes did not vary by group. Thus, NMJs in LA muscles maintained the same relationship between endplate area and TSC number as endplate size changed in response to changing testosterone levels, and this same relationship was seen in EDL muscles. Although mean TSC number also was correlated with mean fiber cross-sectional area in LA muscles ($r^2 = 0.559$; $p < 0.0001$), TSC number and fiber size were not correlated in EDL muscles ($r^2 = 0.021$; $p = 0.46$),

suggesting that fiber size is less tightly linked to TSC number than is terminal size.

DISCUSSION

TSC number is a dynamic feature of the NMJ

Our findings suggest that the number of TSCs present at individual NMJs is dynamic, subject to continual monitoring and alteration. Although TSC number may be relatively constant over short intervals (O'Malley et al., 1999), we have found that TSCs are added as junctions enlarge and lost as junctions shrink. The matching of presynaptic and postsynaptic elements is a critical feature of synaptic development and maintenance and depends to a great extent on intercellular communication. Our data suggest that the third cellular component of the synapse, the TSC, is also regulated in coordination with the presynaptic and postsynaptic cells.

Although altering testosterone levels affected junction size in the highly androgen-sensitive LA muscle but not in the EDL muscle, similar mechanisms appear to regulate TSC numbers in both muscles. Variation was found in EDL junction size, and the slope of the relationship between junction size and TSC number was the same as in LA muscles, even though the variation in EDL junctions was not achieved by manipulating testosterone levels.

The number of Schwann cells associated with axons in peripheral nerve appears to be regulated in a different manner. As nerves lengthen during development, the number of Schwann cells associated with large, myelinated axons actually declines (Berthold and Nilsson, 1987). The distance between nodes of Ranvier increases, and each myelinating Schwann cell becomes responsible for a longer length of axon. In contrast, it appears that each TSC is responsible for a given length of nerve terminal, and as the terminal grows, more TSCs are required. It will be interesting to determine how TSCs divide their coverage of the terminal and how they reorganize as a TSC is added or lost.

What cellular changes and molecular signals underlie changes in TSC number?

The loss of TSCs that occurred when junctions shrank could be attributable to cell death or to the migration of TSCs away from the junction. Similarly, the increase in TSC number that occurred as junctions enlarged could result from division of TSCs at the junction or from Schwann cell migration onto the junction from the nerve. TSC death has been observed after denervation, but only in neonates (Trachtenberg and Thompson, 1996), and TSCs migrate from endplates at long times after denervation of adult muscle (Reynolds and Woolf, 1992). Both cell division and migration participate in the addition of TSCs during early postnatal

development (Love and Thompson, 1998). At present, we cannot distinguish among these possibilities for TSC addition and loss in the adult. We did not observe apoptotic TSC profiles or cells migrating from junctions after castration, nor did we observe mitotic TSCs or cells migrating onto junctions after testosterone treatment. However, given the small numbers of cells added or lost (approximately one cell per endplate) and the short periods required for mitosis or apoptosis, it would probably be difficult to catch cells undergoing either process. Repeated *in vivo* imaging of individual junctions may allow one to observe the change in TSC number as it occurs, perhaps offering insight into the nature of this change.

The testosterone effect on TSC number is likely to be indirect, because TSCs are not thought to express androgen receptors (C. L. Jordan, personal communication). Testosterone probably acts on receptors present in motoneurons and/or muscle fibers (Jordan et al., 1997) to alter junction size, with changes in TSC number occurring secondary to these alterations. It is not clear, however, what signals regulate TSC addition or loss. It is tempting to speculate that some trophic factor furnished to TSCs by nerve terminals regulates TSC number and that the amount of trophic factor provided changes as nerve terminals enlarge or shrink. An attractive candidate for such a trophic factor is neuregulin (Carraway and Burden, 1995), a class of factors expressed by motoneurons and for which Schwann cells possess receptors (Cohen et al., 1992; Marchionni et al., 1993; Ho et al., 1995). Neuregulins have mitogenic and antiapoptotic effects on Schwann cells, as well as effects on Schwann cell motility (Marchionni et al., 1993; Mahanthappa et al., 1996; Trachtenberg and Thompson, 1996, 1997). Another possibility might be neurotransmitter substances released from the nerve terminal, for which TSCs also possess receptors (Son et al., 1996; Araque et al., 1999). Of course, the signal might not come from the nerve terminal at all but rather from the muscle fiber.

What functions do TSCs perform that their number should be so regulated?

Our finding that TSC number is carefully regulated at the NMJ is consistent with an important role for glial cells at the synapse. In addition to modulating the synaptic milieu by buffering ions and taking up neurotransmitters, glial cells are now known to modulate synaptic activity more directly (Araque et al., 1999). For example, TSCs at the frog NMJ regulate the level of synaptic depression produced by high-frequency stimulation (Robitaille, 1998). Such a function may require that an appropriate balance be maintained between the number of release sites (related to terminal size) and TSC number. The fact that TSC number actually decreases when junctions shrink suggests not only that it is important to maintain a minimum number of TSCs at the NMJ, but also that too many TSCs may be detrimental to the normal functioning of this synapse.

REFERENCES

Araque A, Parpura V, Sanzgiri RP, Haydon PG (1999) Tripartite synapses: glia, the unacknowledged partner. Trends Neurosci 22:208–215.

Balice-Gordon RJ, Breedlove SM, Bernstein S, Lichtman JW (1990) Neuromuscular junctions shrink and expand as muscle fiber size is manipulated: *in vivo* observations in the androgen-sensitive bulbocavernosus muscle of mice. J Neurosci 10:2660–2671.

Bebinger DM, Lubischer JL, Thompson WJ (1998) Terminal Schwann cell number in the levator ani muscle, but not the EDL, changes in response to changes in testosterone levels. Soc Neurosci Abstr 24:1546.

Berthold C-H, Nilsson I (1987) Redistribution of Schwann cells in developing feline L7 ventral spinal roots. J Neurocytol 16:811–828.

Bleisch WV, Harrelson A (1989) Androgens modulate endplate size and ACh receptor density at synapses in rat levator ani muscle. J Neurobiol 20:189–202.

Carraway KL, Burden SJ (1995) Neuregulins and their receptors. Curr Opin Neurobiol 5:606–612.

Cohen JA, Yachnis AT, Arai M, Davis JG, Scherer SS (1992) Expression of the *neu* proto-oncogene by Schwann cells during peripheral nerve development and Wallerian degeneration. J Neurosci Res 31:622–634.

Forger NG, Breedlove SM (1987) Seasonal variation in mammalian striated muscle mass and motoneuron morphology. J Neurobiol 18:155–165.

Ho W-H, Armanini MP, Nuijens A, Phillips HS, Osheroff PL (1995) Sensory and motor neuron-derived factor: a novel heregulin variant highly expressed in sensory and motor neurons. J Biol Chem 270:14523–14532.

Jahromi BS, Robitaille R, Charlton MP (1992) Transmitter release increases intracellular calcium in perisynaptic Schwann cells *in situ*. Neuron 8:1069–1077.

Jordan CL, Padgett B, Hershey J, Prins G, Arnold A (1997) Ontogeny of androgen receptor immunoreactivity in lumbar motoneurons and in the sexually dimorphic levator ani muscle of male rats. J Comp Neurol 379:88–98.

Ko C-P, Chen L (1996) Synaptic remodeling revealed by repeated *in vivo* observations and electron microscopy of identified frog neuromuscular junctions. J Neurosci 16:1780–1790.

Love FM, Thompson WJ (1998) Schwann cells proliferate at rat neuromuscular junctions during development and regeneration. J Neurosci 18:9376–9385.

Lubischer JL, Thompson WJ (1999) Neonatal partial denervation results in nodal, but not terminal, sprouting and a decrease in efficacy of remaining neuromuscular junctions in rat soleus muscle. J Neurosci 19:8931–8944.

Mahanthappa NK, Anton ES, Matthew WD (1996) Glial growth factor 2, a soluble neuregulin, directly increases Schwann cell motility and indirectly promotes neurite outgrowth. J Neurosci 16:4673–4683.

Marchionni MA, Goodearl ADJ, Chen MS, Bermingham-McDonogh O, Kirk C, Hendricks M, Danehy F, Misumi D, Sudhalter J, Kobayashi K, Wroblewski D, Lynch C, Baldassare M, Hiles I, Davis JB, Hsuan JJ, Totty NF, Otsu M, McBurney RN, Waterfield MD, Stroobant P, Gwynne D (1993) Glial growth factors are alternatively spliced erbB2 ligands expressed in the nervous system. Nature 362:312–318.

O'Malley JP, Waran MT, Balice-Gordon RJ (1999) In vivo observations of terminal Schwann cells at normal, denervated, and reinnervated mouse neuromuscular junctions. J Neurobiol 38:270–286.

Pfrieger FW, Barres BA (1996) New views on synapse-glia interactions. Curr Opin Neurobiol 6:615–621.

Rance NE, Max SR (1984) Modulation of the cytosolic androgen receptor in striated muscle by sex steroids. Endocrinology 115:862–866.

Reist NE, Smith SJ (1992) Neurally evoked calcium transients in terminal Schwann cells at the neuromuscular junction. Proc Natl Acad Sci USA 89:7625–7629.

Reynolds ML, Woolf CJ (1992) Terminal Schwann cells elaborate extensive processes following denervation of the motor endplate. J Neurocytol 21:50–66.

Rich MM, Lichtman JW (1989) In vivo visualization of pre- and postsynaptic changes during synapse elimination in reinnervated mouse muscle. J Neurosci 9:1781–1805.

Robitaille R (1998) Modulation of synaptic efficacy and synaptic depression by glial cells at the frog neuromuscular junction. Neuron 21:847–855.

Smith ER, Damassa DA, Davidson JM (1978) Hormone administration: peripheral and intracranial implants. In: Methods of psychobiology (Meyer RD, ed), pp 259–279. New York: Academy.

Son Y-J, Trachtenberg JT, Thompson WJ (1996) Schwann cells induce and guide sprouting and reinnervation of neuromuscular junctions. Trends Neurosci 19:280–285.

Trachtenberg JT, Thompson WJ (1996) Schwann cell apoptosis at developing neuromuscular junctions is regulated by glial growth factor. Nature 379:174–177.

Trachtenberg JT, Thompson WJ (1997) Nerve terminal withdrawal from rat neuromuscular junctions induced by neuregulin and Schwann cells. J Neurosci 17:6243–6255.

Wainman P, Shipounoff GC (1941) The effects of castration and testosterone propionate on the striated perinal musculature in the rat. Endocrinology 29:975–978.